

(Modeling of Fluid Phase Equilibria by PC-SAFT EOS)
SOLUBILITY OF GASES/ VAPOR IN POLYETHYLENE

A thesis submitted in partial fulfillment
Of the requirements for the degree of

Bachelor of Technology

In

Chemical Engineering

By

Dibya Lochan Mahapatra (Roll No. 10500032)

Under the supervision of

Dr. Sunil K. Maity



**Department of Chemical Engineering
National Institute of Technology Rourkela**

2009



National Institute of Technology Rourkela

CERTIFICATE

This is to certify that the thesis entitled, “**(Modeling of Fluid Phase Equilibria by Perturbed Chain-Statistical Associating Fluid Theory) SOLUBILITY OF GASES/ VAPOR IN POLYETHYLENE**” submitted by Sri Dibya Lochan Mahapatra in partial fulfillment of the requirements for the award of Bachelor of Technology Degree in Chemical Engineering at National Institute of Technology, Rourkela (Deemed University) is an authentic work carried out by them under my supervision and guidance.

To the best of my knowledge the matter embodied in the thesis has not been submitted to any other University / Institute for the award of any Degree/Diploma.

Date:

Place:

Dr. S. K. Maity

Dept. of Chemical Engineering
National Institute of Technology
Rourkela-769008

ACKNOWLEDGEMENT

I express my sincere gratitude to Dr. S. K. Maity, Professor of the Department of Chemical Engineering, National Institute of Technology, Rourkela, for giving me this great opportunity to work under his guidance throughout the course of this work. I am also thankful to him for his valuable suggestions and constructive criticism which have helped me in the development of this work.

I am also thankful to his optimistic nature which has helped this project to come a long way through.

I also express my sincere gratitude to Prof. R. K. Singh (Chemical Engineering Department, National Institute of Technology, Rourkela) for his coordination in timely completion of the project.

I am also thankful to the Prof K.C.Biswal, Head of the Department, Chemical Engineering for providing me the necessary opportunities for the completion of the project.

Dibya Lochan Mahapatra
(Roll No. 10500032)

CONTENT

	Title	Page No.
	Abstract	i
	List of Figures	ii
	List of Tables	iii
1	INTRODUCTION	1-5
	1.1 Fluid Phase Equilibria	2
	1.2 PC-SAFT Equation Of State	3
	1.3 Objective	5
2	LITERATURE REVIEW	6-10
	2.1 Review of Thermodynamic Models	6
	2.2 Review of Phase Equilibrium Calculation by PC-SAFT EOS	8
3	THEORY	
	3.1 Vapor Liquid Equilibria	11
	3.2 Molecular Model	12
	3.3 Equation of State	13
	3.3.1 Hard-Chain Reference Equation of State	14
	3.3.2 Perturbation Theory for Pure Chain Molecules	14
	3.3.3 Determining Model Constants	16
	3.3.4 Mixtures	18
4	Results and Discussion	20-30
	4.1 Solubility of gases/vapor in ldpe	20
	4.2 Solubility of gases/vapor in hdpe	24

5	Conclusion and Future scope	31
5.1	Conclusion	31
5.2	Future scope	32
	List of symbols	32
	References	34
	Appendix	36

ABSTRACT

The prediction or correlation of thermodynamic properties and phase equilibria with equations of state remains an important goal in chemical and related industries. Although the use of equations of state has for a long time has been restricted to systems of simple fluids, there is an increasing demand for models that are also suitable for complex and macromolecular compounds. Due to its ability to describe the thermodynamics of symmetric as well as asymmetric systems, the most common approaches for modeling gas-polymer solubility have been based on the PC-SAFT EOS. It has wide applicability starting from low molecular weight organic compounds to highly non-ideal macro-molecular weight system such as polymer. In the present work, PC-SAFT equation of state of Gross & Sadowski, 2001 has been used to model solubility of various gases /vapors in liquid polyethylene to demonstrate the suitability of PC-SAFT EOS for polymer-solvent system.

Keywords: PC-SAFT EOS, solubility, phase equilibria.

LIST OF FIGURES

<u>Fig No.</u>	<u>Description</u>	<u>Page No.</u>
1	Liquid–liquid equilibria of polypropylene–n-pentan	9
2	Cloud-point curves of ternary system polypropylene (PP)–n- pentane–CO ₂	10
3	Vapor–liquid phase equilibrium of Polystyrene Chlorobenzene.	10
4	Solubility of ethylene in LDPE	21
5	Solubility of ethylene in LDPE	22
6	Solubility of 1pentene in LDPE	22
7	Solubility of iso-butane in LDPE	23
8	Solubility of cyclo-pentane in LDPE	23
9	Solubility of ethylene in HDPE	26
10	Solubility of ethylene in HDPE	26
11	Solubility of propane in HDPE	27
12	Solubility of isobutane in HDPE	27
13	Solubility of 1-butene in HDPE	28
14	Solubility of CO ₂ in HDPE	28
15	Solubility of CO ₂ in HDPE	29
16	Solubility of N ₂ in HDPE	29
17	Solubility of N ₂ in HDPE	30
18	Solubility of 1octene in HDPE	30

LIST OF TABLES

<u>Table No.</u>	<u>Description</u>	<u>Page No.</u>
1	Universal Model Constants	18

INTRODUCTION

Solubility of gases or vapor in molten polymers is of considerable industrial importance especially for the optimal design of final-treatment processes. The knowledge of the solubility of monomers in polymer is important for understanding processes used for the production, degassing, and subsequent processing. To cover all the conditions met in the process design and operation, thermodynamic models that can be used to describe gas-liquid equilibria (GLE) or vapor-liquid equilibria (VLE) are promising especially when the experimental data are rare.

Most **polyethylene** is manufactured by the high-pressure process at pressures of 2000atm or more. Since conversion of ethylene is never complete, separation equipment is required to separate polyethylene product from unreacted ethylene. Rational design of such equipment requires information on the equilibrium solubility of ethylene in liquid polyethylene at separator conditions. Since direct experimental data are not available, and are difficult to measure, the validated thermodynamic models are quite useful one. In the manufacture of **polyvinyl chloride**, unreacted monomer, vinyl chloride exists in the polymerization products that are harmful to the environment. Devolatilization process is therefore needed to remove those monomers, which needs information of gas solubilities in polymers at various temperatures and pressures.

A further important use of polymers is as membranes for separation of gas mixtures or as barrier membranes to gas transport. An example is the offshore oil and gas industry, which is increasingly turning to the use of flexible flow lines and risers for the development of marginal fields in mature regions and in locations without an established infrastructure. A flexible flow line typically consists of inner and outer polymer tubes (an inner lining and an outer sheath, usually not of the same material) separated by helically wound steel armor. In oil-drilling operations, materials must be able to withstand drilling mud, acid water, and hydrocarbon liquids and gases at pressures up to 1000 bar and temperatures ranging from 4⁰C in the deep sea to 180⁰C in some North Sea wells. The inner liner needs to be resistant to the passage of such gases as carbon dioxide, methane, and hydrogen sulfide, whereas the outer sheath must protect the annulus from sea water

Chapter 1. Introduction

and mechanical impact. The permeation of gases in polymers is a two-step process involving both diffusion of the gas through the polymer and sorption of the gas into the polymer. Experimental data for sorption of gases into polymer is usually scarce, and measurements require considerable experimental effort. Here thermodynamic models can provide powerful tools for modeling and prediction of experimental data (solms et al., 2004).

The sorption of gases in polymers is important in numerous applications, particularly where gas permeability plays an important role. Since the permeability coefficient is the product of the solubility and the diffusion constant, gas sorption is crucial in applications such as gas separation membranes, diffusion barrier materials, polymer foaming processes, and plasticization. Furthermore, O₂ permeability can be the rate determining factor for controlling polymer degradation processes such as oxidation. The purpose of the present investigation is to apply recent Perturbed Chain Statistical Associating Fluid Theory (PC-SAFT) Equation Of State (EOS) of polymers to the problem of calculating the solubility of gases as a function of polymer architecture and solute species.

1.1 Fluid Phase Equilibria

Fluid phase equilibria are of various types

1. Vapor-Liquid equilibria (VLE)
2. Liquid-Liquid equilibria (LLE)
3. Solid-Liquid equilibria (SLE)
4. Solubility of Gases

Of these the solubility of various gases or vapors in polyethylene is of our present interest. The experimental solubility data for various gases and vapors in different polymers are available. However, availability of validated thermodynamic model was found to be very scarce in literature because of complexity involved in the modeling of phase equilibria of polymers systems. There are several challenges involved in the modeling of phase equilibrium of polymers systems.

In the polymerization reaction there are several compounds to consider, depending on the type of reaction, such as polymer, unreacted monomer, and often solvent. The other

Chapter 1. Introduction

compounds that might be present (initiator, surfactant, etc.) can be neglected in terms of phase equilibria as their amount is usually too small to influence it significantly. The processing of the polymer also involves phase equilibria calculations, as the unreacted monomer and the solvent have to be separated from the polymer, usually via flash drums.

The absence of adequate models for the polymer system properties and phase behavior makes this design procedure a time-consuming and costly task that is performed on a trial and-error basis with more art and skilful judgment than solid science. The polymer-solvent phase equilibria is in fact, a very important aspect in the manufacturing, processing, and formulation of polymers. The prediction or correlation of thermodynamic properties and phase equilibria with equations of state remains an important goal in chemical and related industries.

The use of equations of state has been restricted for a quite long time to systems of simple fluids; there is an increasing demand for models that are also suitable for complex and macromolecular compounds like polymers. Subsequently many equation of state was developed for macromolecular compounds based on statistical thermodynamics, such as

- Perturbed Hard Chain Theory.
- Statistical Associating Fluid Theory
- Lennard-Jones Statistical Associating Fluid Theory
- Perturbed Chain Statistical Associating Fluid Theory

Correlation of gas solubility in polymers can also be done using simpler, cubic equations of state such as Sako et al. However, equations of state based on statistical mechanics, such as the SAFT family of equations, offer advantages over purely empirical equations.

1.2 PC-SAFT Equation Of State

For the correlation and prediction of phase equilibrium in macromolecular systems, the equations of state for chain molecules have been successfully used for more than two decades. In many recent investigations, non-spherical molecules are conceived to be chains comprised of freely jointed spherical segments. Several routes have been established to obtain descriptions for those chain fluids. One particularly successful equation of state concept for chain molecules is based on Wertheim's theory of associating fluids. Applying

Chapter 1. Introduction

Wertheim's first-order perturbation theory (TPT1), Chapman et al. derived an equation of state for chain mixtures, known as the statistical associating fluid theory (SAFT). Initially the chain structure was not accounted for in the dispersion term of the SAFT equation, since a hard-sphere reference was used within the chain term; the dispersion contribution of each segment in a chain was assumed to be equal to a non-bonded spherical molecule of the same diameter. Numerous investigators have subsequently examined the use of a square-well reference and a Lennard-Jones reference fluid in the chain-term, leading to equations of state for square-well chains and Lennard-Jones chains, respectively. These expressions are lengthy, and thus many of the most commonly applied engineering equations of state still utilize square-well dispersion terms, which do not account for the connectivity of the segments.

PC-SAFT equation uses the same chain term and association term as the earlier SAFT equations. Because a hard chain fluid serves as a reference for perturbation theory, rather than the spherical molecules as in the SAFT modifications, the proposed model is referred to as perturbed-chain SAFT (PC-SAFT). This model is applicable to real chain molecules of any length, from spheres to polymers.

In the proposed PC-SAFT equation molecules are conceived to be chains composed of spherical segments. Pair potential for the segments of a chain is given by modified square well potential as suggested by [Chen and Kreglewski](#).

$$U(r) = \begin{cases} \infty & r < (\sigma - s_1) \\ 3\varepsilon & (\sigma - s_1) \leq r < \sigma \\ -\varepsilon & \sigma \leq r < \lambda\sigma \\ 0.0 & r \geq \lambda\sigma \end{cases}$$

Where

$U(r)$ is pair potential, r is radial distance between two segments, σ is temp independent segment diameter, ε is the depth of potential well, λ is reduced well width. As suggested by Chen and Kreglewski a ratio of $s_1 / \sigma = 0.12$ is assumed. **Any specific interactions, like hydrogen bonding or dipole-dipole forces have been neglected.** Contributions to the Helmholtz free energy due to such interactions may be implemented separately. According to this model, non associating molecules are characterized by three pure component parameters:

Chapter 1. Introduction

the temp independent segment diameter, σ ; the depth of potential, ϵ ; and the no of segments per chain, m . Additionally PC-SAFT has adjustable solvent-solute binary interaction parameter (K_{ij}) to take into account of interaction of two different segments.

In the present work, PC-SAFT equation of state of [Gross & Sadowski, 2001](#) has been used to model gas-liquid equilibrium since it has wide applicability starting from low molecular weight organic compounds to highly non-ideal macro-molecular weight system such as polymers. The model can also be used to multiple solvent systems and is useful to predict and the solubility at elevated pressure as well. In addition, the PC-SAFT EOS was demonstrated as a useful equation of state for prediction of various thermo-physical properties, such as density, vapour pressure, enthalpy, specific heat capacity etc, of pure components as well as for mixture.

1.3 Objectives

The main objectives of the present work are

- ◆ To develop a generalized thermodynamic model to correlate the solubility of different gases or vapors in polymer.
- ◆ To validate the developed model using literature available data for polyethylene/ solvent (or gas) system.
- ◆ Further objective of the present study is to calculate adjustable binary interaction parameter, K_{ij} , for various polyethylene/ solvent (or gas) systems.

LITERATURE REVIEW

2.1 Review of Thermodynamic Models

One of the recent versions of the SAFT equation of state, PC-SAFT, was first presented [Gross and Sadowski in 2001](#) and has subsequently been applied by Sadowski and co-workers to systems containing polymers; PC-SAFT has also been used by other workers in a number of applications, such as hydrofluoroethers and nitrogen-hydrocarbon systems ([solms et al., 2004](#)). PC-SAFT has also been incorporated into the commercial process simulator Polymers Plus. Results of a study using PC-SAFT to model a polyethylene/ethylene flash in Polymers Plus have appeared recently. Simplified PC-SAFT is an attempt to create a version of PC-SAFT which is both simpler to implement and faster computationally, without sacrificing any of the accuracy of the original equation of state. It is in essence a one-fluid mixing rule applied to PC-SAFT. The result is a simplification of the form of both the chain term and the association contribution to the chemical potential. Simplified PC-SAFT reduces to original PC SAFT in the pure-component limit. Thus there is no need for reparametrization with simplified PC-SAFT, and parameters from the original PC-SAFT papers may thus be used in simplified PC-SAFT. Simplified PC-SAFT has been applied to VLE in polymer systems, LLE in polymer systems, phase equilibrium in the nylon process, and polar systems. In view of the fact that simplified PC-SAFT has already been applied in these different types of systems, it is natural to assess the ability of the model to predict and correlate gas solubility in polymers at high pressures.

Thus PC-SAFT represents an improvement over earlier versions of SAFT by recognizing that **a hard chain is a more appropriate reference system for the chain dispersion contribution than is a mixture of hard spheres**. Such incremental improvements based on molecular theory are not available to empirically derived equations of state.

- ◆ A third advantage is that the SAFT parameters have physical meaning. We have taken advantage of this in two ways.
- ◆ First, by recognizing that segment diameters are similar in nearly all species, from polymers to light gases, we can show that the simplifications made in simplified PC-SAFT (a single average segment diameter for all species in the mixture) do not affect the accuracy of the model.

Chapter 2. Literature Review

- ◆ Second, we can obtain pure-component polymer parameters without the need for binary experimental data. In fact, only limited pure-component experimental data is needed for the polymer.

Knowledge of the phase equilibrium is a prerequisite for the design and optimization of polymer production plants. Modeling the thermodynamic properties of polymer mixtures is demanding in several ways. Two particular aggravations are as follows:

- ❖ First, polymer systems often exhibit pronounced density dependence, where g^E models fail. An equation of state needs to be used instead.
- ❖ Second, experimental data are often scarce. Considerable experimental effort is generally required for determining the high-pressure equilibria of polymer systems. Because measurements are in many cases not available in the literature for a certain condition of interest, it is important from a practical viewpoint that an equation of state is robust for extrapolations beyond the region where parameters were identified.

Physically based equations of state, derived by applying principles of statistical mechanics, have continuously been developed and improved upon over the past 3 decades. Modern equations of state aim at highly nonideal systems, such as polymer mixtures or associating compounds. Reviews on the different lines of development are, e.g., given by [Wei et al., 2000](#) and [Sanchez et al., 1974](#).

In 1988, Chapman et al developed a successful molecular theory, which assumed molecules to be chains of connected spherical segments. Applying Wertheim's thermodynamic perturbation theory of first order (TPT1) and extending it to mixtures, Chapman et al. derived the statistical associating fluid theory (SAFT) equation of state. Huang et al proposed a modification of the SAFT equation of state and determined pure-component parameters for numerous regular as well as polymeric substances. Various modifications of the SAFT model were subsequently suggested. However, SAFT models, other than the version of Huang et al were rarely applied to polymer systems.

In a previous study, the authors have proposed the perturbed-chain SAFT (PC-SAFT) equation of state. The three pure-component parameters required for non associating molecules were determined for numerous substances. The PC-SAFT model was shown to accurately describe vapor pressures, densities, and caloric properties of pure components.

Comparisons to an earlier version of the SAFT equation of state (proposed by Huang et al. revealed a clear improvement for pure-component properties and for vapor–liquid equilibria of mixtures. A brief comparison with the Peng–Robinson model was also given for vapor–liquid equilibria of binary systems, confirming the good performance of the suggested equation of state. In this work, the PC-SAFT equation of state will be utilized to model the phase behavior of binary and ternary systems containing polymers, solvents, and gases.

2.2 Review of Phase Equilibrium Calculation by PC-SAFT EOS

Martin et al., 1999 have published experimental cloud points for polypropylene–n-pentane mixtures. Fig. 1 compares results obtained from the PC-SAFT equation of state with experimental liquid–liquid data at three temperatures. In consideration of a relatively narrow molecular mass distribution, a monodisperse polymer of molecular mass $M = M_w = 50.4$ kg/mol was assumed. The correlation results are in good agreement with the experimental phase behavior using one temperature-independent binary parameter $k_{ij} = 0.0137$.

The use of compressed gases for separating polymers from solvents and for fractioning polymers, as well as the use of supercritical gases as a continuous phase in polymer reactions has given rise for some novel perspectives in process engineering. Martin et al have presented cloud-point measurements for ternary mixtures of polypropylene–n-pentane–CO₂ for various CO₂ contents (Fig. 2). To model this system, the binary k_{ij} parameter for polypropylene–n-pentane is given above ($k_{ij} = 0.0137$) and the binary parameter for n-pentane–CO₂ was set to zero. The k_{ij} parameter between polypropylene and CO₂ was obtained from the ternary mixture, adjusted to the highest point of pressure (at 42 wt.% CO₂, Fig. 8). Applying this approach, PC-SAFT describes the shift of the LCST-demixing (lower critical solution temperature) with varying CO₂ concentrations correctly in Fig. 8 using $k_{ij} = 0$ for the pentane–CO₂ binary and two constant (temperature-independent) k_{ij} parameters.

Fig.3 presents measurements for vapor–liquid mixtures of polystyrene and chloro benzene at $T = 140^\circ\text{C}$ and $T = 160^\circ\text{C}$. The system is well predicted for two temperatures by the PC-SAFT equation of state with $k_{ij}=0$ (5)..

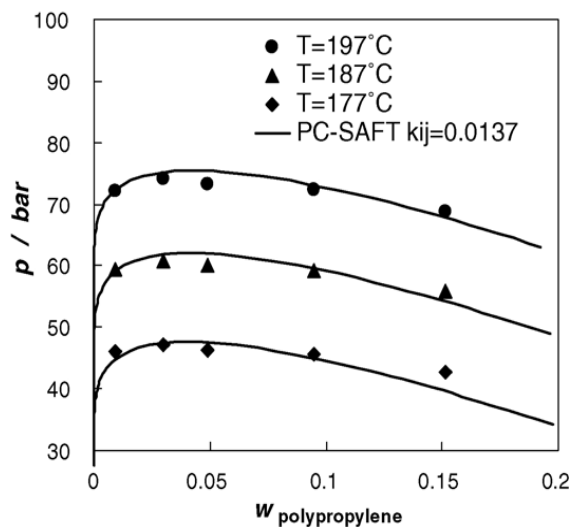


Fig. 1. Liquid-liquid equilibria of polypropylene-n-pentane at three temperatures. Comparison of experimental cloud points to PC-SAFT calculations ($k_{ij} = 0.0137$) assuming that the polymer is monodisperse.

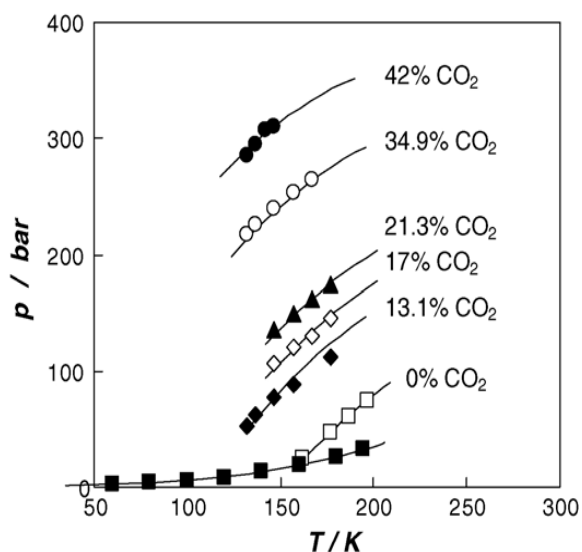


Fig. 2. Cloud-point curves of ternary system polypropylene (PP)-n-pentane-CO₂. Comparison of experimental data to PC-SAFT calculations (PP-n-pentane: $k_{ij} = 0.0137$, PP-CO₂: $k_{ij} = 0.06$, and CO₂-n-pentane: $k_{ij} = 0$).

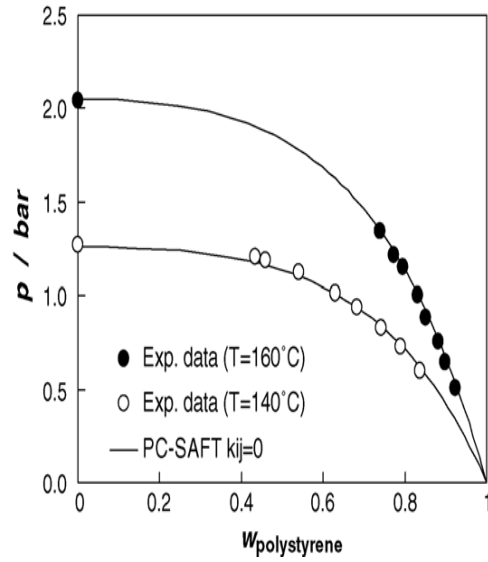


Fig. 3. Vapor–liquid phase equilibrium of polystyrene–chlorobenzene at $T = 140^\circ\text{C}$ and $T = 160^\circ\text{C}$ in a pressure–mass fraction plot. Comparison of experimental data to prediction results of PC-SAFT ($k_{ij} = 0$).

THEORY

In a previous work, an equation of state for square-well chain fluids was derived. This theory will now be extended to real substances. The procedure leading to the equation of state for real substances is similar in spirit to the work of Chen et al. After Alder et al. developed an expression for square-well spheres, Chen and Kreglewski extended the theory to describe real fluids of approximately spherical shape. In this work, we proceed similarly: starting from a theory for square-well chain molecules, we will obtain a model for real chain molecules of any length, from spheres to polymers.

3.1 Gas/Vapor-Liquid Equilibria

For any phase equilibrium, the chemical potential of any component in all the phases are equal under equilibrium condition. For vapor/gas-liquid equilibrium, we can write for a component 'i' as given by the following equation.

$$\mu_i^L = \mu_i^G \quad (1)$$

So applying equilibrium condition

$$\mu_i^0 + RT \ln a_i^L = \mu_i^0 + RT \ln a_i^V \quad (2)$$

$$a_i^L = a_i^V$$

$$\frac{f_i^L}{f_i^0} = \frac{f_i^V}{f_i^0}$$

$$f_i^L = f_i^V \quad (3)$$

Therefore, from the above Eq.3, we conclude that the fugacity of any component in all the phases is equal under equilibrium condition for any phase equilibrium. By using the definition of fugacity, the following equation can be written.

$$\left(\phi_{gas} x_{gas} p \right)^L = \left(\phi_{gas} y_{gas} p \right)^V \quad (4)$$

For solubility of gases or vapors in polymer, we may assume that the liquid polymer remain entirely in the liquid phase because of its high molecular weight. Therefore, the mole fraction of gas/ vapor present in vapor phase is unity. The above equation can be simplified as given by the following equation.

$$x_{gas}^L = \left(\frac{\phi_{gas}^V}{\phi_{gas}^L} \right) \quad (5)$$

Where, x_{gas}^L represents the mole fraction of the gas in polyethylene (liquid phase). In the present work, the values of fugacity coefficients ϕ_{gas}^V and ϕ_{gas}^L were calculated using PC-SAFT equation of state.

3.2 Molecular Model.

In the proposed equation of state, molecules are conceived to be chains composed of spherical segments. The pair potential for the segment of a chain is given by a modified square-well potential, which was suggested by [Chen and Kreglewski](#)

$$u(r) = \begin{cases} \infty & r < (\sigma - s_1) \\ 3\epsilon & (\sigma - s_1) \leq r < \sigma \\ -\epsilon & \sigma \leq r < \lambda\sigma \\ 0 & r \geq \lambda\sigma \end{cases} \quad (6)$$

where $u(r)$ is the pair potential

r is the radial distance between two segments,

σ is the temperature-independent segment diameter,

ϵ denotes the depth of the potential well, and

λ is the reduced well width.

As suggested by [Chen and Kreglewski](#), a ratio of $s_1/\sigma = 0.12$ is assumed.

In contrast to the work of [Chen and Kreglewski](#), no additional temperature correction for the potential depth is introduced. Accordingly, non associating molecules are characterized by three pure-component parameters: the temperature-independent segment diameter σ , the depth of the potential ϵ , and the number of segments per chain m .

Although this potential model is very simple, the step function in the pair potential at $r < \sigma$ accounts for an essential feature of real molecule behavior, the soft repulsion. The soft repulsion is introduced, because molecules have a collision diameter of σ only when they collide at infinitely slow speed (zero temperature limit). Increasing temperature will result in a lower collision diameter.

3.3 Equation of State

According to perturbation theories, the interactions of molecules can be divided into a repulsive part and a contribution due to the attractive part of the potential. To calculate the repulsive contribution, a reference fluid in which no attractions are present is defined. The attractive interactions are treated as a perturbation to the reference system. In the framework of Barker and Henderson's perturbation theory, a reference fluid with hard repulsion and a temperature-dependent segment diameter $d(T)$ can be used to describe the soft repulsion of molecules, where

The reference fluid is given here by the hard-chain fluid and $d(T)$ is the effective collision diameter of the chain segments. For the potential function given in eq 1, integration leads to the temperature-dependent hard segment diameter $d_i(T)$ of component i , according to

$$d_i(T) = \sigma_i \left[1 - 0.12 \exp\left(-\frac{\epsilon_i}{kT}\right) \right] \quad (8)$$

The complete equation of state is given as an ideal gas contribution (id), a hard-chain contribution (hc), and a perturbation contribution, which accounts for the attractive interactions (disp).

$$Z = Z^{\text{id}} + Z^{\text{bc}} + Z^{\text{disp}} \quad (9)$$

where Z is the compressibility factor, with $Z = Pv/(RT)$ and $Z^{\text{id}} = 1$; P is the pressure; v is the molar volume; and R denotes the gas constant. At this point, only dispersive attractions are considered. Specific interactions, such as hydrogen bonding or multipole interactions can be treated separately and will be considered in a subsequent investigation.

3.3.1 Hard-Chain Reference Equation of State

It is based on Wertheim's thermodynamic perturbation theory of first-order, Chapman et al. developed an equation of state, which, for homonuclear hard-sphere chains comprising m segments, is given by

$$Z^{hc} = \bar{m}Z^{hs} - \sum_i x_i(m_i - 1)\rho \frac{\partial \ln g_{ii}^{hs}}{\partial \rho} \quad (10)$$

$$\bar{m} = \sum_i x_i m_i \quad (11)$$

where x_i is the mole fraction of chains of component i , m_i is the number of segments in a chain of component i , ρ is the total number density of molecules, g_{ii}^{hs} is the radial pair distribution function for segments of component i in the hard sphere system, and the superscript hs indicates quantities of the hard-sphere system. Expressions of Boublik and Mansoori et al. are used for mixtures of the hard-sphere reference system in eq 5, given by

$$Z^{hc} = \frac{\zeta_3}{(1 - \zeta_3)} + \frac{3\zeta_1\zeta_2}{\zeta_0(1 - \zeta_3)^2} + \frac{3\zeta_2^3 - \zeta_3\zeta_2^3}{\zeta_0(1 - \zeta_3)^3} \quad (12)$$

$$g_{ij}^{hs} = \frac{1}{(1 - \zeta_3)} + \left(\frac{d_i d_j}{d_i + d_j} \right) \frac{3\zeta_2}{(1 - \zeta_3)} + \left(\frac{d_i d_j}{d_i + d_j} \right)^2 \frac{2\zeta_2^2}{(1 - \zeta_3)^3} \quad (13)$$

Where

$$\zeta_n = \frac{\pi}{6} \rho \sum_i x_i m_i d_i^n \quad n \in \{0, 1, 2, 3\} \quad (14)$$

Note that the compressibility factors of both the hard-chain fluid in eq 5 and the hard-sphere fluid in eq 7 are residual properties, whereas they are often written including the ideal gas contribution in other literature.

3.3.2 Perturbation Theory for Pure Chain Molecules

After the reference chain fluid has been defined (it is identical to the SAFT reference fluid), the perturbation theory of Barker and Henderson can be used to calculate the attractive part of the chain interactions. It is a theory of second order, where the Helmholtz free energy is given as a sum of first- and second-order contributions via

$$\frac{A^{\text{disp}}}{kTN} = \frac{A_1}{kTN} + \frac{A_2}{kTN} \quad (15)$$

Barker and Henderson derived their theory for spherical molecules. This theory can be extended to chain molecules, as each segment of a considered chain is again of spherical shape. The total interaction between two chain molecules required in the perturbation theory is then given by the sum of all individual segment–segment interactions. Chiew obtained expressions for the individual segment–segment radial distribution function ($m; r_{\alpha\beta}, \rho$), which represents the radial distribution function for a segment α of one chain and a segment β of another chain separated by the radial distance $r_{\alpha\beta}$. Chiew also introduced an average inter chain segment–segment radial distribution function $g^{\text{hc}}(m; r, \rho)$, where different segments in a chain are non distinguishable. It is convenient to determine the total interaction between two chains by applying this average radial distribution function. Gross and Sadowski used the results of Chiew and tested the theory for square-well chains. The appropriate equations can easily be written for any potential function as

$$\frac{A_1}{kTN} = -2\pi\rho m^2 \left(\frac{\epsilon}{kT}\right) \sigma^3 \int_1^\infty \tilde{u}(x) g^{\text{hc}}\left(m; x\frac{\sigma}{d}\right) x^2 dx \quad (16)$$

$$\frac{A_2}{kTN} = -\pi\rho m \left(1 + Z^{\text{hc}} + \rho \frac{\partial Z^{\text{hc}}}{\partial \rho}\right)^{-1} m^2 \left(\frac{\epsilon}{kT}\right)^2 \times \quad (17)$$

$$\sigma^3 \frac{\partial}{\partial \rho} \left[\rho \int_1^\infty \tilde{u}(x)^2 g^{\text{hc}}\left(m; x\frac{\sigma}{d}\right) x^2 dx \right]$$

where x is the reduced radial distance around a segment ($x = r/\sigma$), $\tilde{u}(x) = u(x)/\epsilon$ denotes the reduced potential function, and $g^{\text{hc}}(m; x\sigma/d)$ is the average segment–segment radial distribution function of the hard-chain fluid with temperature-dependent segment diameter $d(T)$. The compressibility term in eq 12 can be obtained from eq 5 in the form

$$\left(1 + Z^{\text{hc}} + \rho \frac{\partial Z^{\text{hc}}}{\partial \rho}\right) = \quad (18)$$

$$\left(1 + m \frac{8\eta - 2\eta^2}{(1 - \eta)^4} + (1 - m) \frac{20\eta - 27\eta^2 + 12\eta^3 - 2\eta^4}{[(1 - \eta)(2 - \eta)]^2}\right)$$

where the packing fraction η is equal to $\zeta/3$ defined in eq 9. The packing fraction η represents a reduced segment density.

Expressions for the radial distribution function of the hard-chain system are available in analytic form; however, these expressions are lengthy and lead to tedious calculations here, as an integration over $g^{hc}(r)$ is required in eqs 11 and 12. It is desirable therefore, to simplify the equation of state, and to do so, we first introduce the following abbreviations for the integrals in eq 11 and 12:

$$I_1 = \int_1^\infty \bar{u}(x) g^{hc}\left(m; x\frac{\sigma}{d}\right) x^2 dx \quad (19)$$

$$I_2 = \frac{\partial}{\partial \rho} \left[\rho \int_1^\infty \bar{u}(x)^2 g^{hc}\left(m; x\frac{\sigma}{d}\right) x^2 dx \right] \quad (20)$$

For square-well chains, those integrals are functions of density and segment number only. Formolecules exhibiting soft repulsion, I_1 and I_2 are also functions of temperature. However, the temperature dependence due to $g^{hc}(m; x\sigma/d)$ is moderate and will be neglected here. With this assumption, it is possible to substitute the integrals I_1 and I_2 by power series in density η , where the coefficients of the power series are functions of the chain length.

$$I_1(\eta, m) = \sum_{i=0}^6 a_i(m) \eta^i \quad (21)$$

$$I_2(\eta, m) = \sum_{i=0}^6 b_i(m) \eta^i \quad (22)$$

It was shown earlier that an expression proposed by Liu and Hu captures the dependency of coefficients $a_i(m)$ and $b_i(m)$ upon segment number accurately. It is given by

$$a_i(m) = a_{0i} + \frac{m-1}{m} a_{1i} + \frac{m-1}{m} \frac{m-2}{m} a_{2i} \quad (23)$$

$$b_i(m) = b_{0i} + \frac{m-1}{m} b_{1i} + \frac{m-1}{m} \frac{m-2}{m} b_{2i} \quad (24)$$

These equations were derived from a perturbation theory (sticky-point model based on Cummings and Stell) assuming a correlation of nearest-neighbor segments and next-nearest neighbors. Equations 18 and 19 thus account for the bonding of one segment to a nearest neighbor segment and for the possible bonding of the neighbor segment to a next-nearest neighbor segment.

3.3.3 Determining Model Constants

Let us now be concerned with identifying the model constants a_{0i} , a_{1i} , and a_{2i} as well as b_{0i} , b_{1i} , and b_{2i} of eqs 18 and 19. In a previous work, these constants were obtained by fitting the

eqs 16 and 17 to eqs 14 and 15 for a square-well potential using the radial distribution function proposed by Chiew.²⁸ The appropriate model constants were universal, as the entire ranges for the parameters m and η were covered, i.e., m varies between $m = 1$ for spherical molecules and $m \rightarrow \infty$ for infinitely long chains, and the packing fraction ranges between 0 for an ideal gas and $\eta \leq 0.74$ for the closest packing of segments.

This procedure is, in principle, possible for the potential function given above (eq 1); however, it has proven to be of advantage for an equation of state to incorporate information of real substance behavior. Many of the most successful models derived from statistical mechanics adjusted model constants to pure-component data of real substances. Pure-component data of argon was, for example, used to adjust model constants in Chen and Kreglewski's BACK equation of state. The same dispersion term was also used in the SAFT model of Huang and Radosz. In the case of PHCT, argon and methane served as the model substances. The model constants were in all cases considered to be universal. The reason that this procedure leads to superior models is three-fold: First, there are uncertainties in the dispersion properties, namely, in the assumed perturbing potential $u(x)$ as well as approximations in $g^{hc}(r)$. Second, errors introduced in the reference equation of state can be corrected to a certain extent. Last, the molecular model assuming molecules to be chains of spherical segments might be oversimplified. To correct for these shortcomings, we adjust the model constants a_{0i} , a_{1i} , a_{2i} , b_{0i} , b_{1i} , and b_{2i} to experimental pure-component data. Because the proposed model accounts for the chainlike shape of molecules in the dispersion term, it is essential to include elongated molecules in the fitting procedure, and the series of n-alkanes is best suited to serve as model substances here.

Methane can be assumed to be of spherical shape and will be used to determine the boundary case of $m = 1$, where only the constants a_{0i} and b_{0i} in eqs 18 and 19 are relevant. Our objective is to fit the power-series coefficients of the first-order term a_{0i} , a_{1i} , and a_{2i} as well as those of the second-order term b_{0i} , b_{1i} , and b_{2i} for $i = 1, \dots, 6$ to pure-component data of n-alkanes. To obtain pure-component parameters for the n-alkane components, an intermediate step has to be taken. We have assumed a Lennard-Jones perturbing potential in eqs 14 and 15 and used an expression for the average radial distribution function $g^{hc}(r)$ for hard chains proposed by Chiew. The integral expressions I1 and I2 (eqs 14 and 15) were so determined for Lennard-Jones-like chains. The three pure-component parameters (m , σ , ϵ/k) of the n-alkanes were identified for this equation of state by fitting vapor pressures and PVT data.

In a subsequent step, the coefficients a_{0i} , a_{1i} , a_{2i} , b_{0i} , b_{1i} , and b_{2i} were regressed using the pure-component parameters determined before. Vapor pressures and liquid, vapor, and supercritical volumes were used in the regression, applying a Levenberg–Marquardt algorithm for minimizing the objective function

$$\text{Min} = \sum_{i=1}^{N_{\text{exp}}} \left(\frac{\Omega_i^{\text{exp}} - \Omega_i^{\text{calc}}}{\Omega_i^{\text{exp}}} \right)^2 \quad (25)$$

where (P_{sat}, v) is the vapor pressure or the molar volume and N_{exp} is the total number of experimental points. The results for the coefficients a_{0i} , a_{1i} , and a_{2i} and b_{0i} , b_{1i} , and b_{2i} are given in Table 1. As for the dispersion expression of the BACK equation of state, these values are subsequently treated as universal model constants.

Table 1. Universal Model Constants for Equations 18 and 19

i	a_{0i}	a_{1i}	a_{2i}	b_{0i}	b_{1i}	b_{2i}
0	0.9105631445	-0.3084016918	-0.0906148351	0.7240946941	-0.5755498075	0.0976883116
1	0.6361281449	0.1860531159	0.4527842806	2.2382791861	0.6995095521	-0.2557574982
2	2.6861347891	-2.5030047259	0.5962700728	-4.0025849485	3.8925673390	-9.1558561530
3	-26.547362491	21.419793629	-1.7241829131	-21.003576815	-17.215471648	20.642075974
4	97.759208784	-65.255885330	-4.1302112531	26.855641363	192.67226447	-38.804430052
5	-159.59154087	83.318680481	13.776631870	206.55133841	-161.82646165	93.626774077
6	91.297774084	-33.746922930	-8.6728470368	-355.60235612	-165.2076934	-29.666905585

3.3.4 Mixtures

The perturbation theory of Barker and Henderson, as proposed here, makes use of an average radial distribution function and thus treats the segments of a chain as indistinguishable. Within this concept, a rigorous application of the perturbation theory to mixtures is, in principle, possible. O'Lenick et al. have derived a set of equations for the average radial pair distribution function of mixtures. Unfortunately, these expressions are not available in analytic form. However, the equation of state can easily be extended to mixtures by applying one-fluid mixing rules. Comparisons with simulation data of short-chain mixtures showed that the chain structure does not introduce any significant additional error to the one-fluid mixing rule.

Applying the van der Waals one-fluid mixing rules to the perturbation terms gives

$$\frac{A_1}{kTN} = -2\pi\rho I_1(\eta, \bar{m}) \sum_i \sum_j x_i x_j m_i m_j \left(\frac{\epsilon_{ij}}{kT}\right) \sigma_{ij}^3 \quad (26)$$

$$\begin{aligned} \frac{A_2}{kTN} = & -\pi\rho\bar{m} \left(1 + Z^{\text{hc}} + \rho \frac{\partial Z^{\text{hc}}}{\partial \rho}\right)^{-1} \times \\ & I_2(\eta, \bar{m}) \sum_i \sum_j x_i x_j m_i m_j \left(\frac{\epsilon_{ij}}{kT}\right)^2 \sigma_{ij}^3 \end{aligned} \quad (27)$$

where the power series I1 and I2 (eqs 14 and 15) can now be evaluated for the mean segment number \bar{m} of the mixture, which was given by eq 6. The parameters for a pair of unlike segments are obtained by conventional Berthelot–Lorentz combining rules

$$\sigma_{ij} = \frac{1}{2}(\sigma_i + \sigma_j) \quad (28)$$

$$\epsilon_{ij} = \sqrt{\epsilon_i \epsilon_j} (1 - k_{ij}) \quad (29)$$

where one binary interaction parameter, k_{ij} , is introduced to correct the segment–segment interactions of unlike chains. We also apply the one-fluid mixing concept to the compressibility term in eq 22, i.e., similarly to eq 13, it is

$$\begin{aligned} \left(1 + Z^{\text{hc}} + \rho \frac{\partial Z^{\text{hc}}}{\partial \rho}\right) = & \\ \left(1 + \bar{m} \frac{8\eta - 2\eta^2}{(1 - \eta)^4} + (1 - \bar{m}) \frac{20\eta - 27\eta^2 + 12\eta^3 - 2\eta^4}{[(1 - \eta)(2 - \eta)]^2}\right) & \end{aligned} \quad (30)$$

Equations for pressure, fugacity coefficients, and caloric properties can be derived from the Helmholtz free energy by applying classical thermodynamic relations.

RESULTS AND DISCUSSION

Here in this project work solubility data for different gas and vapor system in LDPE and HDPE having different molecular weight has been considered at various temperatures and pressure and the predicted data from the model has been compared with the experimental data.

4.1 SOLUBILITY OF GASES/VAPOR IN LDPE

Here in this project work solubility data of different gas and vapor system like ethylene, 1-pentene, isobutene, cyclopentane in LDPE system having different molecular weights and at different pressures and temperature has been considered.

Solubility of ethylene in LDPE. The solubility of ethylene in LDPE was reported for two different molecular weight of polyethylene. In both cases it was observed that at a particular temperature solubility of ethylene increases with increase in pressure as shown in [Figure 4](#) and [Figure 5](#). However, the solubility of ethylene was found to decrease with increase in temperature up to the pressure of 220 bar and then increases with increase in temperature for a particular pressure. The PC-SAFT equation was found to correlate the available experimental data suitably with only minor adjustment of K_{ij} . In both cases, estimated optimized K_{ij} values were found to decrease with increase in temperature.

Solubility of 1-pentene in LDPE. The solubility of 1-pentene in polyethylene at two different temperatures was reported. We can see from the figure at a particular temperature solubility of 1-pentene increases with increase in pressure. For 1-pentene solubility was found to be decreasing with increasing temperature. [Figure 6](#) shows the correlated results for the solubilities of 1-pentene in LDPE at various temperatures. From the figure, we can see that the PC-SAFT equation was found to correlate the available experimental data suitably without any adjustment of K_{ij} .

Solubility of isobutane in LDPE. The solubility of isobutane in polyethylene at three different temperatures was reported. We can see from the [Figure 7](#) at a particular temperature

solubility of isobutane increases with increase in pressure. Figure 7 shows the correlated results for the solubilities of 1-pentene in LDPE at various temperatures. The solubility of gas usually decreases with increasing temperature for many gas-polymer systems. For isobutane also the solubility decreases with increasing temperature. PC-SAFT equation was found to correlate the available experimental data suitably with only a minor adjustment of K_{ij} . In this case, estimated optimized K_{ij} value was found to be decreasing first as the temp increased but then again increased with further increase in temperature.

Solubility of cyclo-pentane in LDPE. The solubility of cyclo-pentane in LDPE was reported at two different temperatures. In this case it was observed that at a particular temperature solubility of cyclo-pentane increases with increase in pressure as shown in Figure 8. The PC-SAFT equation was found to correlate the available experimental data suitably with out any adjustment of K_{ij} .

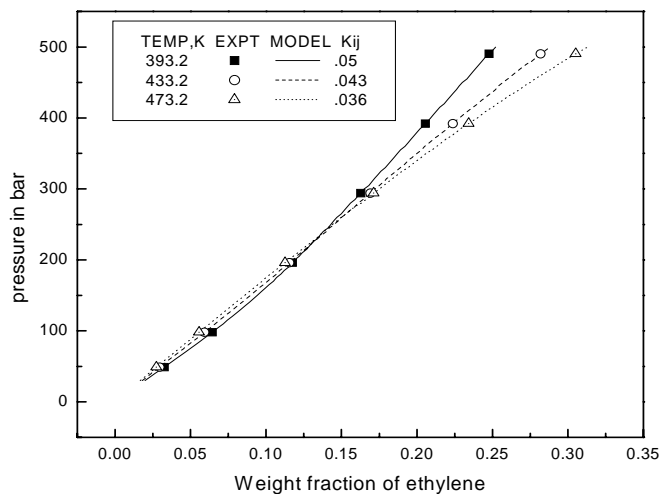


Figure 4. Solubility of ethylene in LDPE. Conditions: $M_n/\text{kg.mol}^{-1} = 3.65$, $M_w/\text{kg.mol}^{-1} = 7.6$ [Kobyakov et al, 1987].

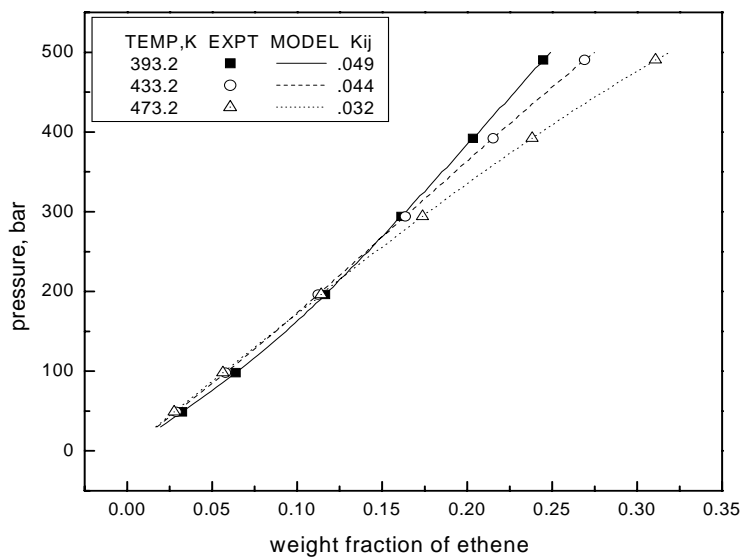


Figure 5. Solubility of ethene in LDPE. Conditions: $M_n/\text{kg}\cdot\text{mol}^{-1} = 4.95$, $M_w/\text{kg}\cdot\text{mol}^{-1} = 11.0$ [Kobyakov et al, 1987].

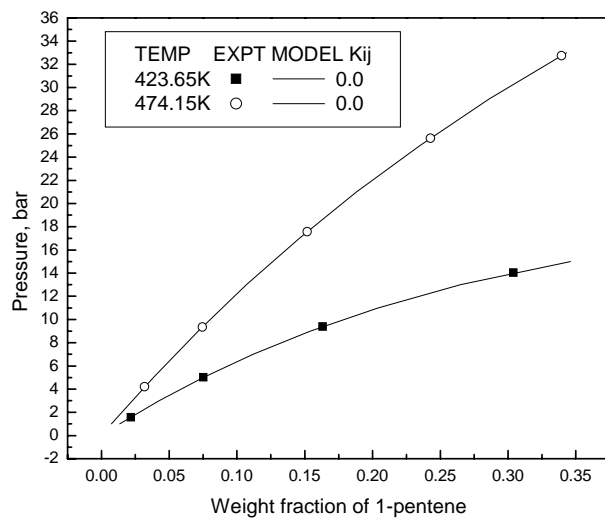


Figure 6. Solubility of 1-pentene in LDPE. Conditions: $M_n/\text{kg}\cdot\text{mol}^{-1} = 76$, LDPE, MI = 65, $\rho = 0.919 \text{ g/cm}^3$ [Surana et al, 1997].

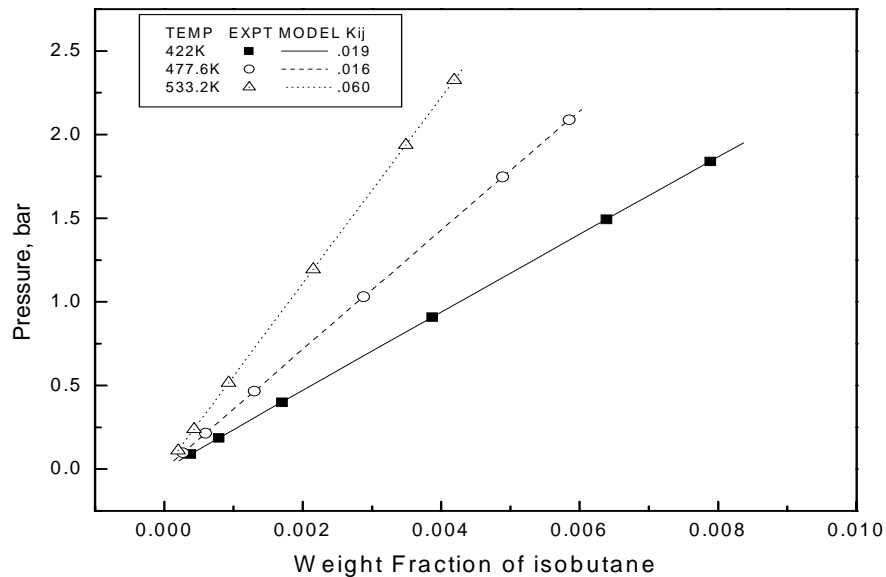


Figure 7. Solubility of isobutane in LDPE. Conditions: $M_n/\text{kg.mol}^{-1} = 18$, $M_w/\text{kg.mol}^{-1} = 109$, $\rho = 0.919 \text{ g/cm}^3$ [Meyer et al, 1983].

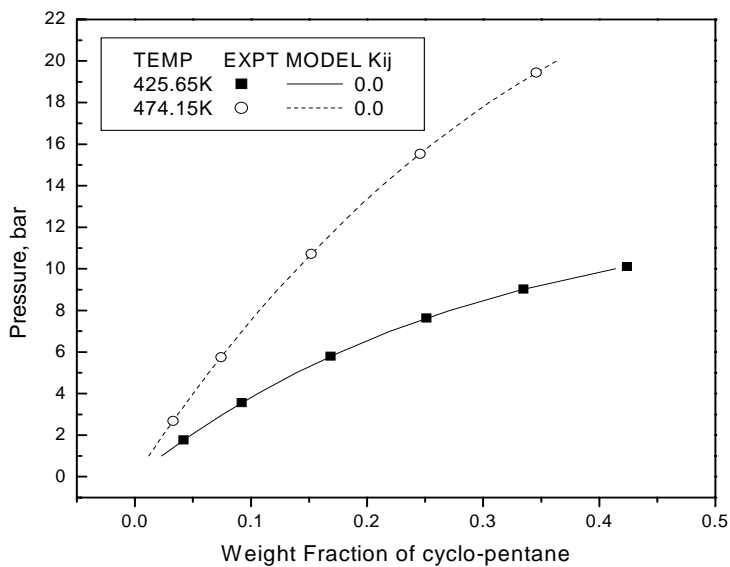


Figure 8. Solubility of cyclo-pentane in LDPE. Conditions: $M_n/\text{kg.mol}^{-1} = 76$, $MI = 65$, $\rho = 0.919 \text{ g/cm}^3$ [Surana et al, 1997].

4.2 SOLUBILITY OF GASES/VAPOR IN HDPE

Here in this project work solubility data of different gas and vapor system like ethylene, propane, isobutane, 1-butene, nitrogen, carbon dioxide, 1-octene in HDPE system having different molecular weights and at different pressures and temperature has been considered.

Solubility of ethylene in HDPE. The solubility of ethylene in HDPE was reported for two different molecular weight of polyethylene. In both cases it was observed that at a particular temperature solubility of ethylene increases with increase in pressure as shown in [Figure 9](#) and [Figure 10](#). The solubility of ethylene was found to decrease with increase in temperature. The PC-SAFT equation was found to correlate the available experimental data suitably with only minor adjustment of K_{ij} . In both cases, estimated optimized K_{ij} values were initially found to be increasing with increase in temperature then decreasing with increase in temperature

Solubility of propane in HDPE. The solubility of propane in HDPE was reported at three different temperatures. Solubility of propane was found to be increasing with increase in pressure as shown in [Figure 11](#). The solubility of propane was found to be decreasing with increase in temperature. The PC-SAFT equation was found to correlate the available experimental data suitably with only minor adjustment of K_{ij} . Estimated optimized K_{ij} value was found to be decreasing with increase in temperature.

Solubility of isobutane in HDPE. The solubility of isobutane in HDPE was reported at three different temperatures. Solubility of isobutane was found to be increasing with increase in pressure as shown in [Figure 12](#). The solubility of isobutane was found to be decreasing with increase in temperature. The PC-SAFT equation was found to correlate the available experimental data suitably with only minor adjustment of K_{ij} . Estimated optimized K_{ij} value was found to be first increasing with increasing in temperature then decreasing with increase in further temperature.

Solubility of 1-butene in HDPE. The solubility of 1-butene in HDPE was reported at constant temperatures. Solubility of 1-butene was found to be increasing with increase in pressure as shown in [Figure 13](#). The PC-SAFT equation was found to correlate the available experimental data suitably with only minor adjustment of K_{ij} .

Solubility of CO₂ in HDPE. The solubility of CO₂ in HDPE was reported for two different molecular weight of polyethylene. In both cases it was observed that at a particular temperature solubility of CO₂ increases with increase in pressure as shown in [Figure 14](#) and [Figure 15](#). However, the solubility of CO₂ was found to increase with increase in temperature for the first case and decrease with increase in temperature for the second case for a particular pressure. The PC-SAFT equation was found to correlate the available experimental data suitably with very less adjustment of Kij. In the first case estimated optimized Kij values were found to decrease with decrease in temperature while in the second case Kij values were found to increase with increase in temperature.

Solubility of N₂ in HDPE. . The solubility of N₂ in HDPE was reported for two different molecular weight of N₂ at three different temperatures. In both cases it was observed that at a particular temperature solubility of N₂ increases with increase in pressure as shown in [Figure 16](#) and [Figure 17](#). However, the solubility of N₂ was found to increase with increase in temperature at a particular pressure. The PC-SAFT equation was found to correlate the available experimental data suitably with very less adjustment of Kij. In both the cases estimated optimized Kij values were found to increase first and then decrease with increase in temperature.

Solubility of 1-octene in HDPE. The solubility of 1-octene in HDPE was reported at two different temperatures. Solubility of 1-octene was found to be increasing with increase in pressure as shown in [Figure 18](#). The PC-SAFT equation was found to correlate the available experimental data suitably with only minor adjustment of Kij. Estimated optimized Kij was found to be constant with increase in temperature.

Results And Discussion

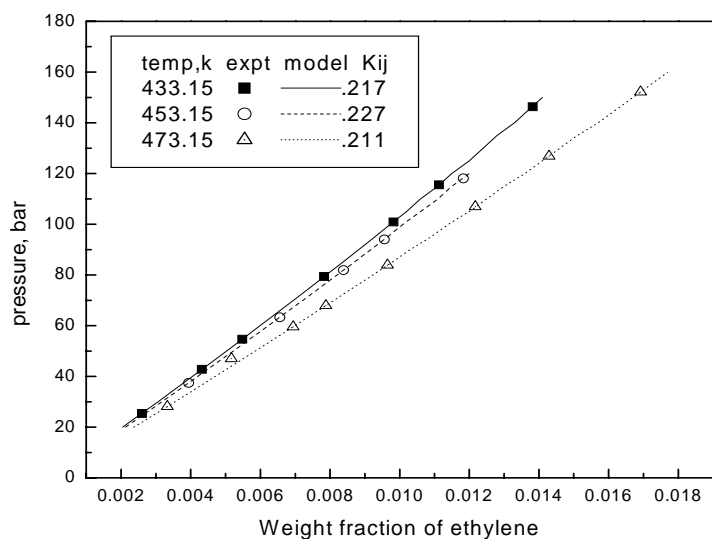


Figure 9. Solubility of ethylene in HDPE. Conditions: $M_n/\text{kg.mol}^{-1} = 8.2$, $M_w/\text{kg.mol}^{-1} = 111.0$, [Sato et al, 1999].

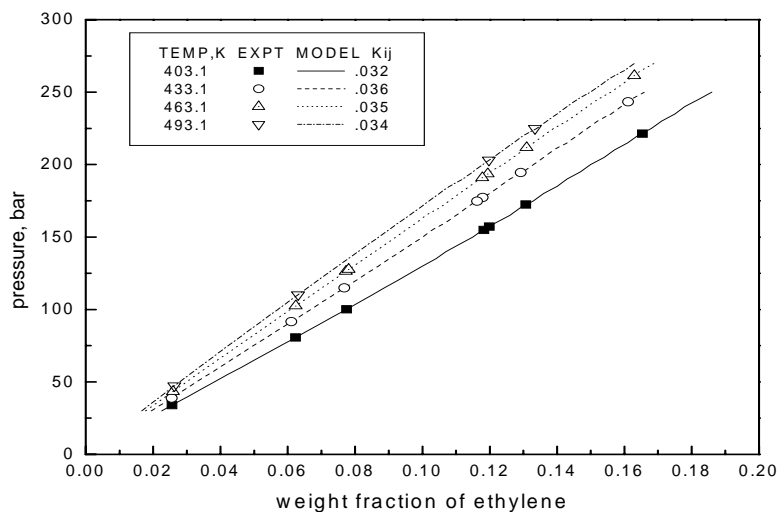


Figure 10. Solubility of ethylene in HDPE. Conditions: $M_n/\text{kg.mol}^{-1} = 2.2$, $M_w/\text{kg.mol}^{-1} = 2.4$, [Rousseaux et al, 1985].

Results And Discussion

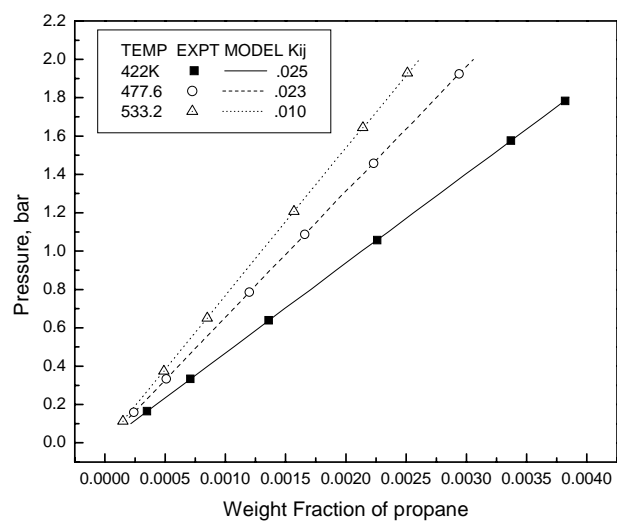


Figure 11. Solubility of propane in HDPE. Conditions: $M_n/\text{kg.mol}^{-1} = 14$, $M_w/\text{kg.mol}^{-1} = 94$, $\rho = 0.951 \text{ g/cm}^3$ [Meyer and Blanks, 1983].

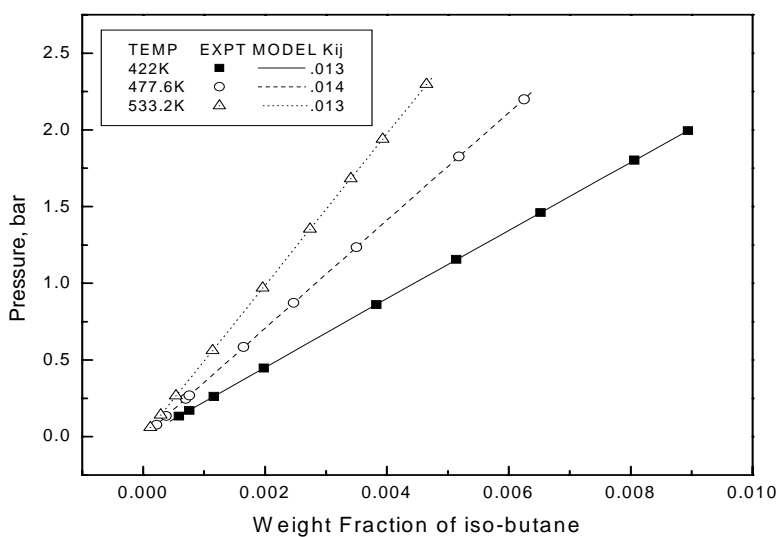


Figure 12. Solubility of isobutane in HDPE. Conditions: $M_n/\text{kg.mol}^{-1} = 14$, $M_w/\text{kg.mol}^{-1} = 94$, $\rho = 0.951 \text{ g/cm}^3$, [Meyer and Blanks, 1983].

Results And Discussion

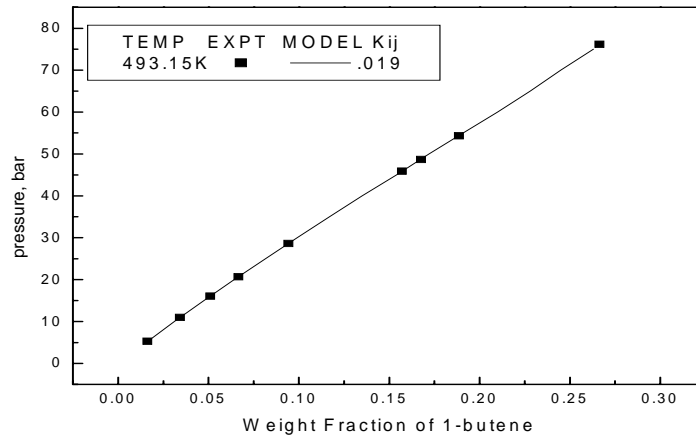


Figure 13. Solubility of 1-butene in HDPE. Conditions: $M_n/\text{kg.mol}^{-1} = 43$, $M_w/\text{kg.mol}^{-1} = 105$, $M_z/\text{kg.mol}^{-1} = 190$, [Tork, T, 2001].

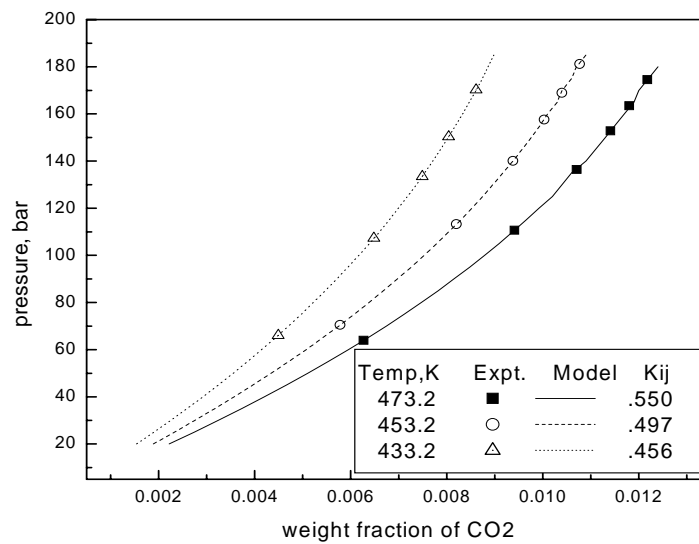


Figure 14. Solubility of CO₂ in HDPE. Conditions: $M_w = 1.11 \times 10^5$, $M_w/M_n = 13.6$, $T_m = 402\text{K}$. [Sato et al, 1999].

Results And Discussion

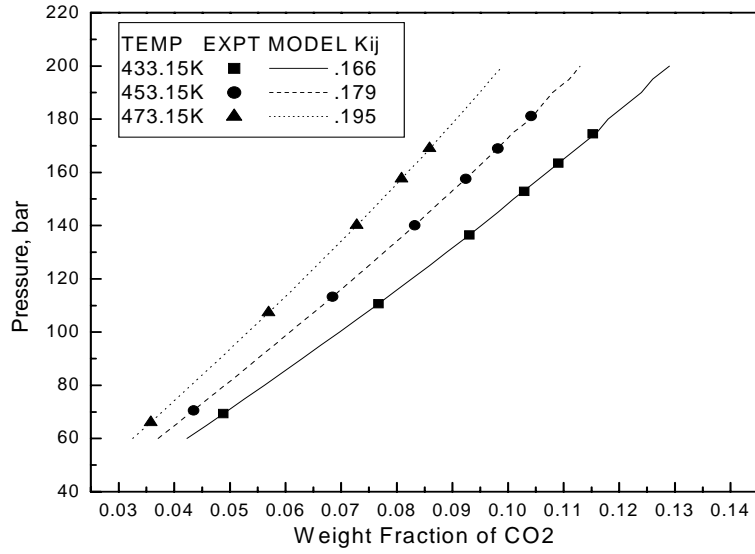


Figure 15. Solubility of CO₂ in HDPE. Conditions: Mn=8200, Mw=111,000, [Sato et al, 1999].

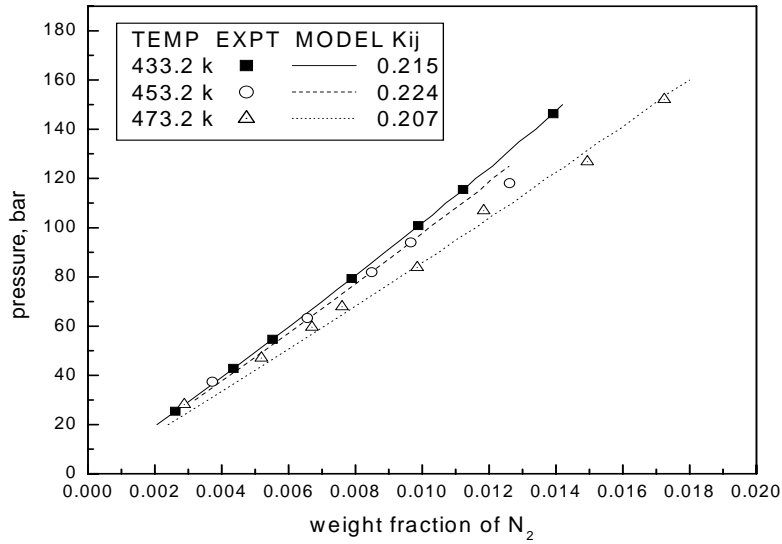


Figure 16. Solubility of N₂ in HDPE. Conditions: Mw=1.11×10⁵, Mw/Mn=13.6, Tm=402 K [Sato et al, 1999].

Results And Discussion

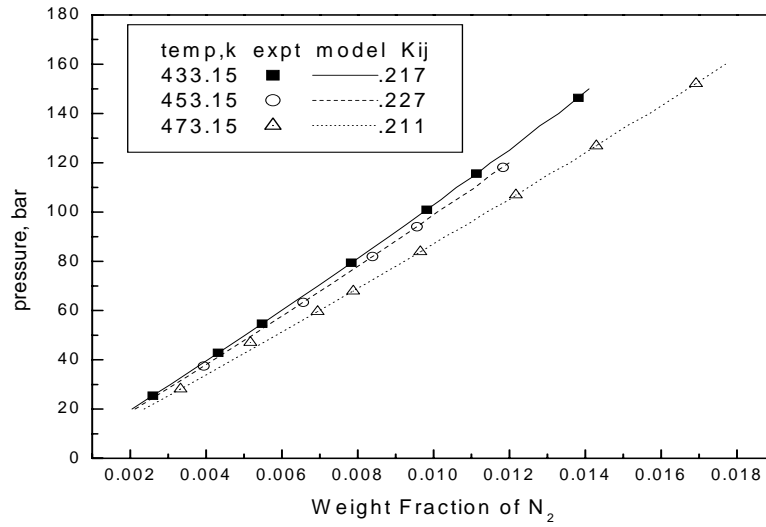


Figure 17. Solubility of N₂ in HDPE. Conditions: $M_n/\text{kg.mol}^{-1} = 8.2$, $M_w/\text{kg.mol}^{-1} = 111$ [Sato et al, 1999].

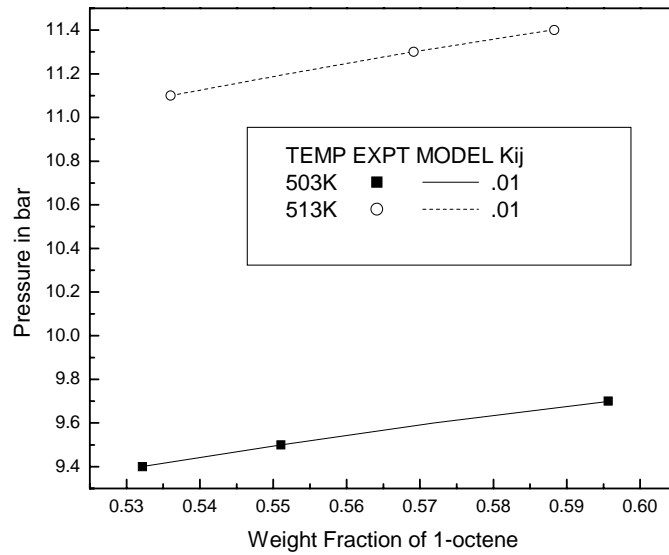


Figure 18. Solubility of 1-octene in HDPE. Conditions: $M_n/\text{kg.mol}^{-1} = 43$, $M_w/\text{kg.mol}^{-1} = 105$, $M_z/\text{kg.mol}^{-1} = 190$ [Tork, T, 2001].

CONCLUSION AND FUTURE SCOPE

5.1 CONCLUSION

We have successfully modeled gas solubilities in various polymers at high temperatures and pressures using simplified PC-SAFT. Usually a temperature independent value of the binary interaction parameter k_{ij} is required to correlate experimental data successfully. In this contribution we have shown that PC-SAFT is suitable for compounds of any molar mass, from gases to polymers as well as for polar and associating substances and their mixtures. When applied to vapor–liquid equilibria the PC-SAFT equation of state shows substantial predictive capabilities and good correlation results. Both, vapor/gas–liquid were correlated using one temperature-independent binary interaction parameter (k_{ij}). The PC-SAFT equation of state was found to give good correlation results and can safely extrapolate and even predict the phase behavior of various complex systems over wide ranges of conditions.

5.2 FUTURE SCOPE

The PC-SAFT model can also be used for modeling of fluid phase equilibria in case of multi component systems. it can also be used for modeling of other polymer systems. Calculation of Pressure, Density, Fugacity Coefficients, and Caloric Properties can also be done using the Perturbed-Chain SAFT Model.

LIST OF SYMBOLS

A = Helmholtz free energy, J
 A_1 = Helmholtz free energy of first-order perturbation term, J
 A_2 = Helmholtz free energy of second-order perturbation term, J
 a_{01}, a_{02}, a_{03} = model constants; defined in eq 18
 $a_j(m)$ = functions defined by eqs 18 and 19
 b_{01}, b_{02}, b_{03} = model constants defined in eq 19
 d = temperature-dependent segment diameter, A
 g_{hc} = average radial distribution function of hard-chain fluid
= site-site radial distribution function of hard-chain fluid
 I_1, I_2 = abbreviations defined by eqs 14–17
 k = Boltzmann constant, J/K
 k_{ij} = binary interaction parameter
 K = K factor, $K_i = y_i/x_i$
 m = number of segments per chain
 m^+ = mean segment number in the system, defined in eq 6
 M = molar mass, g/mol
 N = total number of molecules
 P = pressure, Pa
 R = gas constant, J mol⁻¹ K⁻¹
 r = radial distance between two segments, A
 s_1 = constant defining the pair potential, defined in eq 1, A
 T = temperature, K
 $u(r)$ = pair potential function, J
 v = molar volume, m³/mol
 x = reduced radial distance between two segments
 x_i = mole fraction of component i
 Z = compressibility factor

Greek Letters

ε = depth of pair potential, J
 η = packing fraction, $\eta = \zeta^3$ (see eq 9)
 λ = reduced well width of square-well potential
 ρ = total number density of molecules, 1/A³

σ = segment diameter, A

ζ_n = abbreviation ($n = 0, \dots, 3$) defined by eq 9, An-3

Superscripts

calc = calculated property

crit = critical property

disp = contribution due to dispersive attraction

exp = experimental property

hc = residual contribution of hard-chain system

hs = residual contribution of hard-sphere system

id = ideal gas contribution

REFERENCES

1. Solms, N.Von; Nielsen, J.K.; Hassager, O.; Rubin, A.; Dandekar, A.Y.; Andersen, S.I.; Stenby, E.H. Direct measurement of gas solubility in polymers with a high-pressure microbalance. *Journal of Applied Polymer Science*, 2004, 91, 1476–1488.
2. Wei, Y. S.; Sadus, R. J. Equations of State for the Calculation of Fluid-Phase Equilibria. *AIChE J.*, 2000, 46, 169.
3. Sanchez, I. C.; Lacombe, R. H. Theory of liquid-liquid and liquid-vapor equilibria. *Nature (London)*, 1974, 252, 381.
4. Joachim Gross and Gabriele Sadowski, Modeling polymer system using the perturbed-chain statistical associating fluid theory equation of state. *Ind. Eng. Chem. Res.* 2001, 40, 1244-1260.
5. Martin, T. M.; Lateef, A. A.; Roberts, C. B. Measurements and modeling of cloud point behavior for polypropylene/*n*-pentane and polypropylene/*n*-pentane/carbon dioxide mixtures at high pressures. *Fluid Phase Equilib.* 1999, 154, 241.
6. Sako, T.; Wu, A. H.; Prausnitz, J. M. A Cubic Equation of State for High-Pressure phase-Equilibria of Mixtures Containing Polymers and Volatile Fluids. *J. Appl. Polym. Sci.* 1989, 38, 1839.
7. Nuno Pedrosa; Lourdes F. Vega; Joo A. P.; Coutinho; Isabel M. Marrucho. Phase equilibria calculations of polyethylene solutions from saft-type equations of state. *Macromolecules*, 2006, 39 (12), 4240-4246.
8. Steven J. Moore; Sieghard E. Wanke. Solubility of ethylene, 1-butene and 1-hexene in polyethylenes. *Chemical Engineering Science* 2001, 56, 4121–4129.
9. Dennis P. Maloney; John M. Prausnitz. Solubility of ethylene in liquid, low density polyethylene at industrial-separation pressures. *Ind. Eng. Chem. Process Des. Dev.*, 1976, 15 (1), 216-220.
10. Solms N. von; Michelsen L. Michael; Kontogeorgis M. Georgios; Prediction and correlation of high-pressure gas solubility in polymers with simplified pc-saft. *Ind. Eng. Chem. Res.*, 2005, 44 (9), 3330-3335.
11. Rousseaux, P.; Richon, D.; Renon, H.. Ethylene-polyethylene mixtures, saturated liquid densities and bubble pressures up to 26.1 MPa and 493.1 K, *J. Polym. Sci.: Polym. Chem. Ed.*, 23, 1771-1985.

12. Y. Sato, K. Fujiwara, T. Takikawa, Sumarno, S. Takishima, H. Masuoka, Solubilities and diffusion coefficients of carbon dioxide and nitrogen in polypropylene, high-density polyethylene, and polystyrene under high pressures and temperatures. *Fluid Phase Equilibria* 162,1999, 261–276.
13. Kobaykov, V.M., Kogan, V.B., and Zernov, V.S., Metod otsenki dannykh o parozhidkostnom ravnovesii pri vysokikh davleniyakh, *Zh. Prikl. Khim.*, 60, 81, 1987.
14. Surana, R.K., Danner, R.P., DeHaan, A.B., and Beckers, N., New technique to measure high-pressure and high-temperature polymer-solvent vapor-liquid equilibrium, *Fluid Phase Equil.*, 139, 361, 1997
15. Tork, T., Measurement and calculation of phase equilibria in polyolefin/solvent systems (Ger.), Dissertation, TU Berlin, 2001.
16. Meyer, J.A.; Blanks, R.F., Solubility of isobutane and propane in polyethylene at high temperatures and low pressures, *J. Appl. Polym. Sci.*, 28, 725, 1983.
17. Gross, J.; Sadowski, G. Application of perturbation theory to a hard-chain reference fluid: An equation of state for squarewell chains. *Fluid Phase Equilib.* **2000**, 168, 183.
18. Chen, S. S.; Kreglewski, A. Applications of the Augmented van der Waals Theory of Fluids. I. Pure Fluids. *Ber. Bunsen-Ges.* **1977**, 81 (10), 1048.

APPENDIX

PC-SAFT MODEL

Due to its ability to describe the thermodynamics of symmetric as well as asymmetric systems, the most common approaches for modeling fluid phase equilibria in case of polymer system solubility have been based on the PC-SAFT EOS. This model not only gives the best result but also is very simple to use by developing a computer based general methodology for PC-SAFT EOS. This equation of state requires three pure component parameters: segment number (m), segment diameter (σ), and energy parameter (ε/κ). Additionally PC-SAFT has adjustable solvent-solute binary interaction parameter (K_{ij}).

Summary of Equations

This section provides a summary of equations for calculating thermo physical properties like pressure, density, fugacity coefficients, and caloric properties using the perturbed-chain SAFT equation of state. The Helmholtz free energy A_{res} is the starting point in this paragraph, as all other properties can be obtained as derivatives of A_{res} . In the following, a tilde ($\tilde{}$) will be used for reduced quantities, and caret symbols ($\hat{}$) will indicate molar quantities. The reduced Helmholtz free energy, for example, is given by

$$\tilde{a}^{res} = \frac{A^{res}}{NkT} \quad (\text{A.1})$$

At the same time, one can write in terms of the molar quantity

$$\tilde{a}^{res} = \frac{\hat{a}^{res}}{RT} \quad (\text{A.2})$$

Helmholtz Free Energy

The residual Helmholtz free energy consists of the hard-chain reference contribution and the dispersion contribution

$$\tilde{a}^{res} = \tilde{a}^{hc} + \tilde{a}^{disp} \quad (\text{A.3})$$

Hard-Chain Reference Contribution

$$\tilde{a}^{hc} = \bar{m}\tilde{a}^{hs} - \sum_i x_i(m_i - 1) \ln g_{ii}^{hs}(\sigma_{ii}) \quad (\text{A.4})$$

where m^+ is the mean segment number in the mixture

Appendix

$$\bar{m} = \sum_i x_i m_i \quad (\text{A.5})$$

The Helmholtz free energy of the hard-sphere fluid is given on a per-segment basis

$$\begin{aligned} \bar{a}^{\text{hs}} &= \frac{A^{\text{hs}}}{N_s kT} \\ &= \frac{1}{\zeta_0} \left[\frac{3\zeta_1 \zeta_2}{(1 - \zeta_3)} + \frac{\zeta_2^3}{\zeta_3 (1 - \zeta_3)^2} + \left(\frac{\zeta_2^3}{\zeta_3^2} - \zeta_0 \right) \ln(1 - \zeta_3) \right] \end{aligned} \quad (\text{A.6})$$

and the radial distribution function of the hard-sphere fluid is

$$\begin{aligned} g_{ij}^{\text{hs}} &= \frac{1}{(1 - \zeta_3)} + \left(\frac{d_i d_j}{d_i + d_j} \right) \frac{3\zeta_2}{(1 - \zeta_3)^2} + \\ &\quad \left(\frac{d_i d_j}{d_i + d_j} \right)^2 \frac{2\zeta_2^2}{(1 - \zeta_3)^3} \end{aligned} \quad (\text{A.7})$$

with ζ_n defined as

$$\zeta_n = \frac{\pi}{6} \rho \sum_i x_i m_i d_i^n \quad n \in \{0, 1, 2, 3\} \quad (\text{A.8})$$

The temperature-dependent segment diameter d_i of component i is given by

$$d_i = \sigma_i \left[1 - 0.12 \exp\left(-3 \frac{\epsilon_i}{kT}\right) \right] \quad (\text{A.9})$$

Dispersion Contribution

The dispersion contribution to the Helmholtz free energy is given by

$$\bar{a}^{\text{disp}} = -2\pi\rho I_1(\eta, \bar{m}) \overline{m^2 \epsilon \sigma^3} - \pi\rho\bar{m} C_1 I_2(\eta, \bar{m}) \overline{m^2 \epsilon^2 \sigma^3} \quad (\text{A.10})$$

where we have introduced an abbreviation C_1 for the compressibility expression, which is defined as

$$\begin{aligned} C_1 &= \left(1 + Z^{\text{hc}} + \rho \frac{\partial Z^{\text{hc}}}{\partial \rho} \right)^{-1} \\ &= \left(1 + \bar{m} \frac{8\eta - 2\eta^2}{(1 - \eta)^4} + \right. \\ &\quad \left. (1 - \bar{m}) \frac{20\eta - 27\eta^2 + 12\eta^3 - 2\eta^4}{[(1 - \eta)(2 - \eta)]^2} \right) \end{aligned} \quad (\text{A.11})$$

We have also introduced the abbreviations

Appendix

$$\overline{m^2 \epsilon \sigma^3} = \sum_i \sum_j x_i x_j m_i m_j \left(\frac{\epsilon_{ij}}{kT} \right) \sigma_{ij}^3 \quad (\text{A.12})$$

$$\overline{m^2 \epsilon^2 \sigma^3} = \sum_i \sum_j x_i x_j m_i m_j \left(\frac{\epsilon_{ij}}{kT} \right)^2 \sigma_{ij}^3 \quad (\text{A.13})$$

Conventional combining rules are employed to determine the parameters for a pair of unlike segments.

$$\sigma_{ij} = \frac{1}{2}(\sigma_i + \sigma_j) \quad (\text{A.14})$$

$$\epsilon_{ij} = \sqrt{\epsilon_i \epsilon_j} (1 - k_{ij}) \quad (\text{A.15})$$

The integrals of the perturbation theory are substituted by simple power series in density

$$I_1(\eta, \bar{m}) = \sum_{i=0}^6 a_i(\bar{m}) \eta^i \quad (\text{A.16})$$

$$I_2(\eta, \bar{m}) = \sum_{i=0}^6 b_i(\bar{m}) \eta^i \quad (\text{A.17})$$

where the coefficients a_i and b_i depend on the chain length according to

$$a_i(\bar{m}) = a_{0i} + \frac{\bar{m} - 1}{\bar{m}} a_{1i} + \frac{\bar{m} - 1}{\bar{m}} \frac{\bar{m} - 2}{\bar{m}} a_{2i} \quad (\text{A.18})$$

$$b_i(\bar{m}) = b_{0i} + \frac{\bar{m} - 1}{\bar{m}} b_{1i} + \frac{\bar{m} - 1}{\bar{m}} \frac{\bar{m} - 2}{\bar{m}} b_{2i} \quad (\text{A.19})$$

The universal model constants for the a_{0i} , a_{1i} , a_{2i} , b_{0i} , b_{1i} , and b_{2i} are given in Table 1.

Density

The density at a given system pressure P_{sys} must be determined iteratively by adjusting the reduced density η until $P_{\text{calc}} = P_{\text{sys}}$. A suitable starting value for a liquid phase is $\eta = 0.5$; for a vapor phase, $\eta = 10^{-10}$. Values of $\eta > 0.7405$ [$= \pi/(3\sqrt{2})$] are higher than the closest packing of segments and have no physical relevance. The number density of molecules ρ is calculated from η through

$$\rho = \frac{6}{\pi} \eta \left(\sum_i x_i m_i d_i^3 \right)^{-1} \quad (\text{A.20})$$

The quantities ζ_n given in eq A.8 can now be calculated. For a converged value of η , we obtain the molar density ρ , in units of kmol/m³, from

$$\hat{\rho} = \frac{\rho}{N_{\text{AV}}} \left(10^{10} \frac{\text{\AA}}{\text{m}} \right)^3 \left(10^{-3} \frac{\text{kmol}}{\text{mol}} \right) \quad (\text{A.21})$$

where ρ is, according to eq A.20, given in units of A-3 and $NAV = 6.022 \times 10^{23} \text{ mol}^{-1}$ denotes Avogadro's number.

Pressure

Equations for the compressibility factor will be derived using the thermodynamic Relation

$$Z = 1 + \eta \left(\frac{\partial \tilde{a}^{\text{res}}}{\partial \eta} \right)_{T, x_i} \quad (\text{A.22})$$

The pressure can be calculated in units of Pa = N/m² by applying the relation

$$P = ZkT\rho \left(10^{10} \frac{\text{\AA}}{\text{m}} \right)^3 \quad (\text{A.23})$$

From eqs A.22 and A.3, it is

$$Z = 1 + Z^{\text{hc}} + Z^{\text{disp}} \quad (\text{A.24})$$

Hard-Chain Reference Contribution

The residual hard-chain contribution to the compressibility factor is given by

$$Z^{\text{hc}} = \bar{m}Z^{\text{hs}} - \sum_i x_i (m_i - 1) (g_{ii}^{\text{hs}})^{-1} \rho \frac{\partial g_{ii}^{\text{hs}}}{\partial \rho} \quad (\text{A.25})$$

where Z^{hs} is the residual contribution of the hard-sphere fluid, given by

$$Z^{\text{hs}} = \frac{\zeta_3}{(1 - \zeta_3)} + \frac{3\zeta_1\zeta_2}{\zeta_0(1 - \zeta_3)^2} + \frac{3\zeta_2^3 - \zeta_3\zeta_2^3}{\zeta_0(1 - \zeta_3)^3} \quad (\text{A.26})$$

$$\begin{aligned} \rho \frac{\partial g_{ij}^{\text{hs}}}{\partial \rho} &= \frac{\zeta_3}{(1 - \zeta_3)^2} + \left(\frac{d_i d_j}{d_i + d_j} \right) \left(\frac{3\zeta_2}{(1 - \zeta_3)^2} + \frac{6\zeta_2\zeta_3}{(1 - \zeta_3)^3} \right) + \\ &\quad \left(\frac{d_i d_j}{d_i + d_j} \right)^2 \left(\frac{4\zeta_2^2}{(1 - \zeta_3)^3} + \frac{6\zeta_2^2\zeta_3}{(1 - \zeta_3)^4} \right) \quad (\text{A.27}) \end{aligned}$$

and was given in eq A.7.

Dispersion Contribution

The dispersion contribution to the compressibility factor can be written as

$$\begin{aligned} Z^{\text{disp}} &= -2\pi\rho \frac{\partial(\eta I_1)}{\partial \eta} \overline{m^2 \epsilon \sigma^3} - \\ &\quad \pi\rho\bar{m} \left[C_1 \frac{\partial(\eta I_2)}{\partial \eta} + C_2 \eta I_2 \right] \overline{m^2 \epsilon^2 \sigma^3} \quad (\text{A.28}) \end{aligned}$$

Where

$$\frac{\partial(\eta I_1)}{\partial \eta} = \sum_{j=0}^6 a_j(\bar{m})(j+1)\eta^j \quad (\text{A.29})$$

$$\frac{\partial(\eta I_2)}{\partial \eta} = \sum_{i=0}^6 b_j(\bar{m})(j+1)\eta^j \quad (\text{A.30})$$

and where C2 is an abbreviation defined as

$$C_2 = \frac{\partial C_1}{\partial \eta} = -C_1^2 \left(\bar{m} \frac{-4\eta^2 + 20\eta + 8}{(1-\eta)^5} + (1-\bar{m}) \frac{2\eta^3 + 12\eta^2 - 48\eta + 40}{[(1-\eta)(2-\eta)]^3} \right) \quad (\text{A.31})$$

Fugacity Coefficient

The fugacity coefficient $k(T,P)$ is related to the residual chemical potential according to

$$\ln \varphi_k = \frac{\mu_k^{\text{res}}(T,v)}{kT} - \ln Z \quad (\text{A.32})$$

The chemical potential can be obtained from

$$\frac{\mu_k^{\text{res}}(T,v)}{kT} = \bar{a}^{\text{res}} + (Z-1) + \left(\frac{\partial \bar{a}^{\text{res}}}{\partial x_k} \right)_{T,v,x_{i \neq k}} - \sum_{j=1}^N x_j \left[\left(\frac{\partial \bar{a}^{\text{res}}}{\partial x_j} \right)_{T,v,x_{i \neq j}} \right] \quad (\text{A.33})$$

where derivatives with respect to mole fractions are calculated regardless of the summation relation $\sum x_j = 1$. For convenience, one can define abbreviations for derivatives of eq A.8 with respect to mole fraction.

$$\zeta_{n,xk} = \left(\frac{\partial \zeta_n}{\partial x_k} \right)_{T,\rho,x_{j \neq k}} = \frac{\pi}{6} \rho m_k (d_k)^n \quad n \in \{0, 1, 2, 3\} \quad (\text{A.34})$$

Hard-Chain Reference Contribution

$$\left(\frac{\partial \bar{a}^{\text{hc}}}{\partial x_k} \right)_{T,\rho,x_{j \neq k}} = m_k \bar{a}^{\text{hs}} + \bar{m} \left(\frac{\partial \bar{a}^{\text{hs}}}{\partial x_k} \right)_{T,\rho,x_{j \neq k}} - \sum_i x_i (m_i - 1) (g_{ii}^{\text{hs}})^{-1} \left(\frac{\partial g_{ii}^{\text{hs}}}{\partial x_k} \right)_{T,\rho,x_{j \neq k}} \quad (\text{A.35})$$

Appendix

$$\begin{aligned}
\left(\frac{\partial \bar{a}}{\partial x_k}\right)_{T,\rho,x_{j \neq k}}^{\text{hs}} &= -\frac{\zeta_{0,xk}}{\zeta_0} \bar{a}^{\text{hs}} + \frac{1}{\zeta_0} \left[\frac{3(\zeta_{1,xk}\zeta_2 + \zeta_1\zeta_{2,xk})}{(1-\zeta_3)} + \right. \\
&\quad \frac{3\zeta_1\zeta_2\zeta_{3,xk}}{(1-\zeta_3)^2} + \frac{3\zeta_2^2\zeta_{2,xk}}{\zeta_3(1-\zeta_3)^2} + \frac{\zeta_2^3\zeta_{3,xk}(3\zeta_3-1)}{\zeta_3^2(1-\zeta_3)^3} + \\
&\quad \left. \left(\frac{3\zeta_2^2\zeta_{2,xk}\zeta_3 - 2\zeta_2^3\zeta_{3,xk}}{\zeta_3^3} - \zeta_{0,xk} \right) \ln(1-\zeta_3) + \right. \\
&\quad \left. \left(\zeta_0 - \frac{\zeta_2^3}{\zeta_3} \right) \frac{\zeta_{3,xk}}{(1-\zeta_3)} \right] \quad (\text{A.36})
\end{aligned}$$

$$\begin{aligned}
\left(\frac{\partial g_{ij}^{\text{hs}}}{\partial x_k}\right)_{T,\rho,x_{j \neq k}} &= \frac{\zeta_{3,xk}}{(1-\zeta_3)^2} + \\
&\quad \left(\frac{d_i d_j}{d_i + d_j} \right) \left(\frac{3\zeta_{2,xk}}{(1-\zeta_3)^2} + \frac{6\zeta_2\zeta_{3,xk}}{(1-\zeta_3)^3} \right) + \\
&\quad \left(\frac{d_i d_j}{d_i + d_j} \right)^2 \left(\frac{4\zeta_2\zeta_{2,xk}}{(1-\zeta_3)^3} + \frac{6\zeta_2^2\zeta_{3,xk}}{(1-\zeta_3)^4} \right) \quad (\text{A.37})
\end{aligned}$$

Dispersion Contribution

$$\begin{aligned}
\left(\frac{\partial \bar{a}}{\partial x_k}\right)_{T,\rho,x_{j \neq k}}^{\text{hs}} &= -2\pi\rho [I_{1,xk} \overline{m^2 \epsilon \sigma^3} + I_1 \overline{(m^2 \epsilon \sigma^3)_{xk}}] - \\
&\quad \pi\rho \{ [m_k C_1 I_2 + \bar{m} C_{1,xk} I_2 + \bar{m} C_1 I_{2,xk}] \overline{m^2 \epsilon^2 \sigma^3} + \\
&\quad \bar{m} C_{1,I_2} \overline{(m^2 \epsilon^2 \sigma^3)_{xk}} \} \quad (\text{A.38})
\end{aligned}$$

$$\overline{(m^2 \epsilon \sigma^3)_{xk}} = 2m_k \sum_j x_j m_j \left(\frac{\epsilon_{kj}}{kT} \right) \sigma_{kj}^3 \quad (\text{A.39})$$

$$\overline{(m^2 \epsilon^2 \sigma^3)_{xk}} = 2m_k \sum_j x_j m_j \left(\frac{\epsilon_{kj}}{kT} \right)^2 \sigma_{kj}^3 \quad (\text{A.40})$$

$$\begin{aligned}
C_{1,xk} &= C_2 \zeta_{3,xk} - \\
C_1 &\left\{ m_k \frac{8\eta - 2\eta^2}{(1-\eta)^4} - m_k \frac{20\eta - 27\eta^2 + 12\eta^3 - 2\eta^4}{[(1-\eta)(2-\eta)]^2} \right\} \quad (\text{A.41})
\end{aligned}$$

$$I_{1,xk} = \sum_{i=0}^6 [a_i(\bar{m}) i \zeta_{3,xk} \eta^{i-1} + a_{i,xk} \eta^i] \quad (\text{A.42})$$

$$I_{2,xk} = \sum_{i=0}^6 [b_i(\bar{m}) i \zeta_{3,xk} \eta^{i-1} + b_{i,xk} \eta^i] \quad (\text{A.43})$$

$$a_{i,xk} = \frac{m_k}{\bar{m}^2} a_{1i} + \frac{m_k}{\bar{m}^2} \left(3 - \frac{4}{\bar{m}} \right) a_{2i} \quad (\text{A.44})$$

$$b_{i,xk} = \frac{m_k}{\bar{m}^2} b_{1i} + \frac{m_k}{\bar{m}^2} \left(3 - \frac{4}{\bar{m}} \right) b_{2i} \quad (\text{A.45})$$

Enthalpy and Entropy

The molar enthalpy \hat{h}^{res} is obtained from a derivative of the Helmholtz free energy with respect to temperature, according to

$$\frac{\hat{h}^{\text{res}}}{RT} = -T \left(\frac{\partial \bar{a}^{\text{res}}}{\partial T} \right)_{\rho, x_i} + (Z - 1) \quad (\text{A.46})$$

Unlike the enthalpy of an ideal gas, which is a function of temperature only, the entropy of an ideal gas is a function of both temperature and pressure (or density). Hence, the residual entropy in the variables P and T is different from the residual entropy for the specified conditions of v and T. It is

$$\frac{\hat{s}^{\text{res}}(P, T)}{R} = \frac{\hat{s}^{\text{res}}(v, T)}{R} + \ln(Z) \quad (\text{A.47})$$

All of the equations for \bar{a}^{res} are given in the variables v and T, so that the residual entropy can be written as

$$\frac{\hat{s}^{\text{res}}(P, T)}{R} = -T \left[\left(\frac{\partial \bar{a}^{\text{res}}}{\partial T} \right)_{\rho, x_i} + \frac{\bar{a}^{\text{res}}}{T} \right] + \ln(Z) \quad (\text{A.48})$$

The residual molar Gibbs free energy $\hat{g}^{\text{res}}(P, T)$ is defined as

$$\frac{\hat{g}^{\text{res}}}{RT} = \frac{\hat{h}^{\text{res}}}{RT} - \frac{\hat{s}^{\text{res}}(P, T)}{R} \quad (\text{A.49})$$

or simply as

$$\frac{\hat{g}^{\text{res}}}{RT} = \bar{a}^{\text{res}} + (Z - 1) - \ln(Z) \quad (\text{A.50})$$

The temperature derivative of \bar{a}^{res} in eqs A.46 and A.48 is again the sum of two contributions

$$\left(\frac{\partial \bar{a}^{\text{res}}}{\partial T} \right)_{\rho, x_i} = \left(\frac{\partial \bar{a}^{\text{hc}}}{\partial T} \right)_{\rho, x_i} + \left(\frac{\partial \bar{a}^{\text{disp}}}{\partial T} \right)_{\rho, x_i} \quad (\text{A.51})$$

With abbreviations for two temperature derivatives

$$d_{i,T} = \frac{\partial d_i}{\partial T} = \sigma_i \left(3 \frac{\epsilon_i}{kT^2} \right) \left[-0.12 \exp \left(-3 \frac{\epsilon_i}{kT} \right) \right] \quad (\text{A.52})$$

$$\zeta_{n,T} = \frac{\partial \zeta_n}{\partial T} = \frac{\pi}{6} \rho \sum_i x_i m_i n d_{i,T} (d_i)^{n-1} \quad n \in \{1, 2, 3\} \quad (\text{A.53})$$

the hard-chain contribution and the dispersion contribution can conveniently be written.

Hard-Chain Reference Contribution

$$\left(\frac{\partial \bar{a}^{\text{hc}}}{\partial T} \right)_{\rho, x_i} = \bar{m} \left(\frac{\partial \bar{a}^{\text{hs}}}{\partial T} \right)_{\rho, x_i} - \sum_i x_i (m_i - 1) (g_{ii}^{\text{hs}})^{-1} \left(\frac{\partial g_{ii}^{\text{hs}}}{\partial T} \right)_{\rho, x_i} \quad (\text{A.54})$$

Appendix

$$\begin{aligned} \left(\frac{\partial \bar{a}^{hs}}{\partial T}\right)_{\rho, x_i} &= \frac{1}{\zeta_0} \left[\frac{3(\zeta_{1,T}\zeta_2 + \zeta_1\zeta_{2,T})}{(1-\zeta_3)} + \frac{3\zeta_1\zeta_2\zeta_{3,T}}{(1-\zeta_3)^2} + \right. \\ &\quad \left. \frac{3\zeta_2^2\zeta_{2,T}}{\zeta_3(1-\zeta_3)^2} + \frac{\zeta_2^3\zeta_{3,T}(3\zeta_3-1)}{\zeta_3^2(1-\zeta_3)^3} + \right. \\ &\quad \left. \left(\frac{3\zeta_2^2\zeta_{2,T}\zeta_3 - 2\zeta_2^3\zeta_{3,T}}{\zeta_3^3} \right) \ln(1-\zeta_3) + \left(\zeta_0 - \frac{\zeta_2^3}{\zeta_3^2} \right) \frac{\zeta_{3,T}}{(1-\zeta_3)} \right] \end{aligned} \quad (\text{A.55})$$

Equation A.54 requires only the i - i pairs in the temperature derivative of the radial pair distribution function. For simplicity, one can restrict oneself to the i - i pairs in eq A.7 by equating

$$\frac{1}{2}d_i = \left(\frac{d_i d_i}{d_i + d_i} \right) \quad (\text{A.56})$$

The temperature derivative of the radial pair distribution function is then

$$\begin{aligned} \frac{\partial g_{ii}^{hs}}{\partial T} &= \frac{\zeta_{3,T}}{(1-\zeta_3)^2} + \left(\frac{1}{2}d_{i,T} \right) \frac{3\zeta_2}{(1-\zeta_3)^2} + \\ &\quad \left(\frac{1}{2}d_i \right) \left(\frac{3\zeta_{2,T}}{(1-\zeta_3)^2} + \frac{6\zeta_2\zeta_{3,T}}{(1-\zeta_3)^3} \right) + \left(\frac{1}{2}d_i d_{i,T} \right) \frac{2\zeta_2^2}{(1-\zeta_3)^3} + \\ &\quad \left(\frac{1}{2}d_i \right)^2 \left(\frac{4\zeta_2\zeta_{2,T}}{(1-\zeta_3)^3} + \frac{6\zeta_2^2\zeta_{3,T}}{(1-\zeta_3)^4} \right) \end{aligned} \quad (\text{A.57})$$

Dispersion Contribution.

$$\begin{aligned} \left(\frac{\partial \bar{a}^{disp}}{\partial T}\right)_{\rho, x_i} &= -2\pi\rho \left(\frac{\partial I_1}{\partial T} - \frac{I_1}{T} \right) \overline{m^2 \epsilon \sigma^3} - \\ &\quad \pi\rho\bar{m} \left[\frac{\partial C_1}{\partial T} I_2 + C_1 \frac{\partial I_2}{\partial T} - 2C_1 \frac{I_2}{T} \right] \overline{m^2 \epsilon^2 \sigma^3} \end{aligned} \quad (\text{A.58})$$

with

$$\frac{\partial I_1}{\partial T} = \sum_{i=0}^6 a_i(\bar{m}) i \zeta_{3,T} \eta^{i-1} \quad (\text{A.59})$$

$$\frac{\partial I_2}{\partial T} = \sum_{i=0}^6 b_i(\bar{m}) i \zeta_{3,T} \eta^{i-1} \quad (\text{A.60})$$

$$\frac{\partial C_1}{\partial T} = \zeta_{3,T} C_2 \quad (\text{A.61})$$

Correlations for Pure-Component Parameters

Equation 18, which was given the purpose of model development, is a well suitable function for correlating pure-component parameters with varying segment number. It is suitable, because it allows for varying parameters of short chains but converges to constant values as

Appendix

segment number increases. Generally, this equation captures the effect of chain length on physical properties. It is convenient, though, to modify this equation to obtain a correlation of pure component parameters with molar mass, rather than with varying segment number. For convenience, we choose the molar mass of one hydrocarbon unit to be equal to the molar mass of methane ($M_{CH_4} = 16.043$ g/mol) and obtain the following relation for the segment diameter of the n-alkane series:

$$\sigma_i = q_{01} + \frac{M_i - M_{CH_4}}{M_i} q_{11} + \frac{M_i - M_{CH_4}}{M_i} \frac{M_i - 2M_{CH_4}}{M_i} q_{21} \quad (B.1)$$

For the ratio of the segment number to the molar mass (m_i/M_i) and the energy parameter ϵ_i/k of the n-alkanes, we obtain

$$(m_i/M_i) = q_{02} + \frac{M_i - M_{CH_4}}{M_i} q_{12} + \frac{M_i - M_{CH_4}}{M_i} \frac{M_i - 2M_{CH_4}}{M_i} q_{22} \quad (B.2)$$

$$(\epsilon_i/k) = q_{03} + \frac{M_i - M_{CH_4}}{M_i} q_{13} + \frac{M_i - M_{CH_4}}{M_i} \frac{M_i - 2M_{CH_4}}{M_i} q_{23} \quad (B.3)$$

where q_{jk} are constants that can be fitted to the pure-component parameter.

For the n-alkane series, these constants are

j	units	0	1	2
q_{j1}	Å	3.7039	-0.3226	0.6907
q_{j2}	mol/g	0.06233	-0.02236	-0.01563
q_{j3}	K	150.03	80.68	38.96